X-ray scatter data for diagnostic radiology

1978 Phys. Med. Biol. 23 1076

(http://iopscience.iop.org/0031-9155/23/6/003)

PHYS. MED. BIOL., 1978, Vol. 23, No. 6, 1076–1085. Printed in Great Britain

X-ray Scatter Data for Diagnostic Radiology

C. E. DICK, PH.D., C. G. SOARES, PH.D. and J. W. MOTZ, PH.D.

National Bureau of Standards, Washington, DC 20234, U.S.A.

Received 30 *December* 1977, *in final form* 28 *March* 1978

ABSTRACT. The ratio of the scattered to the total X-ray fluence (scatter fraction) at the centre of the image plane for X-rays transmitted through polystyrene phantoms has been measured for X-ray energies of 32 and 69 keV, X-ray beam diameters from 4 to 40 cm, phantom thicknesses from 5 to 30 cm and phantom-to-image-plane separations from 0·3 to 40 cm. The experimental values for this ratio have less than a 10% variation for these two X-ray energies and the experimental data show good agreement with Monte Carlo calculations and available experimental results for low atomic number materials. Based on these results, simple curves are generated which give estimates (±10%) of the scatter fraction for all combinations of the geometric parameters encountered in diagnostic radiology.

1. Introduction

In diagnostic radiology, the X-rays transmitted through the patient to the image plane consist of an unscattered and a scattered component. In order to estimate the effect of the scattered X-rays on the quality of the radiographic image, it is necessary to determine the values of these two components.

As shown in previous studies (Motz and Dick 1975, Motz and Danos 1977) the effect of the scattered radiation on the image information content may be expressed in terms of the scatter fraction F, defined as

$$F = N_s/(N_u + N_s) \tag{1}$$

where N_u and N_s are the unscattered and scattered X-ray fluences (number per unit area) at a specified point in the image plane. The determination of the scatter fraction F is complicated by the fact that it depends on several variables, including the incident X-ray energy, the diameter W of the X-ray beam incident on the phantom, the thickness L of the phantom under investigation, the separation distance H between the exit surface of the phantom and the image plane and the density and atomic number of the material being examined. In the present study, scatter effects will be measured only for polystyrene which approximates the scattering cross-sections for muscle tissue in the energy range 30–70 keV (Hubbell 1969).

Experimental and theoretical studies of scattered X-rays (Meakin 1957, Halmshaw 1966, Goodwin, Quimby and Morgan 1970, Reiss and Steinle 1973, Motz and Dick 1975, Stargardt and Angerstein 1975, Brueckner 1977, private communication) have been made for applications in both industrial and medical radiography. In general, these data have been incomplete since the dependence of the scatter fraction on all of the scatter parameters has not been determined. In addition, the results have been inconsistent, particularly in

0031–9155/78/0006–1076 $02.00

determining the dependence of the scatter fraction on the incident X-ray energy. In order to resolve these differences, the dependence of the scatter fraction has been examined for a range of values of all of the above geometric parameters which apply to the conditions that are usually found in diagnostic radiology.

2. Experimental arrangement and procedure

The experimental set-up utilised in these measurements is shown in fig. 1. Monoenergetic X-ray beams with energies of 32 and 69 keV produced by a method previously described (Motz and Dick 1975) were incident on polystyrene

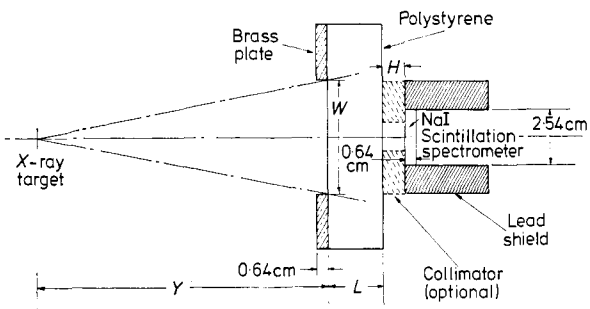

Fig. 1. The experimental arrangement used for the determination of the scatter fraction F from polystyrene phantoms. Note that the optional collimator is not used in the present experiment but is shown because of its implications for previous measurements (Motz and Dick 1975).

scattering phantoms of thickness L. The exit surface of these phantoms was located at a distance $Y+L$ from the X-ray target and a distance H from the face of a 2·5 cm diameter by 0·64 cm thick NaI scintillation spectrometer. The X-ray beam incident on the polystyrene was collimated to a diameter W by circular holes machined in 0·64 cm thick brass plates. This set-up differs from our previous measurements (Motz and Dick 1975) in that (a) for these measurements the beam diameter was defined by the brass plates at the incident surface of the polystyrene and (b) no collimation is used in front of the scintillation spectrometer. The collimator shown by the dashed lines in fig. 1 was used in our previous measurements, and the significance of omitting this collimator will be discussed in Section 4.

Output pulses from the scintillation spectrometer were recorded by a conventional multichannel analyser. In all of the measurements described below, the X-ray fluence incident on the polystyrene was determined by monitoring the electron beam charge incident on the X-ray target and by correcting for electronic dead time in the counting circuitry.

For a given set of values for the parameters of interest, the scatter fraction F was determined by measuring pulse height spectra for the following cases for X-ray beam energies of 32 and 69 keV:

(a) The incident X-ray fluence N_0 was measured with the detector collimated with a 0·3 cm diameter lead aperture 0·3 cm thick and no scatterer in place.

The front surface of the scintillator was placed at a location corresponding to a distance H from the exit plane of the phantom. The X-ray fluence at the location of the image plane was determined by integrating these spectra in a manner similar to that previously described (Motz and Dick 1975) and by dividing by the area of the collimator. For a range of H values from 0 to 40 cm these data agree with an inverse square law dependence to $\pm 2\%$.

(b) The unscattered X-ray fluence N_u through a phantom of thickness L was determined by repeating the measurements described above for each thickness of scatterer used. The value of the linear attenuation coefficient derived from these two measurements agree with tabulated values (Hubbell 1969) for polystyrene to $\pm 2\%$.

(c) The total X-ray fluence $(N_u + N_s)$ transmitted through the phantom was determined from the pulse height spectra recorded for given values of L, W and H with no collimation between the phantom and the detector.

From these measurements, the scatter fraction F is determined from eqn (1). Although the measurements (a) and (b) are redundant, both were made to ensure that the collimator used in (b) was small enough so that the value of N_u did not include any scatter contribution. The uncertainty in the value of F determined by this technique is estimated to be $\pm 5\%$, as based on statistical counting uncertainties in the determination of N_u and $(N_u + N_s)$.

3. Results

Measurements of the scatter fraction F were made for a wide range of values of the above parameters which are sufficient to encompass most cases encountered in a radiographic situation. In particular, F was determined for the parameter values given in table 1 for the two X-ray energies, 32 and 69 keV.

Table 1. Values of the geometric parameters†

$Y+L$ (cm)	L (cm)	W (cm)	H (cm)
250	5	3·7, 7, 10	0·3, 0·1W,
	10	14, 25	0·5W, W
	21		
	29		
400	5		0·3, 0·1W,
	10	40	
	21		0·5W, W

† These parameters are defined in fig. 1.

Two values of the X-ray target to phantom distance $(Y+L)$ were used in order to increase conveniently the beam diameter from 25 to 40 cm. Also, the scatter fraction for $L = 29$ was determined only at 69 keV due to the high absorption of 32 keV X-rays in this thickness of material.

3.1. *Dependence of the scatter fraction on the beam diameter and the patient thickness*

The dependence of F on the parameters W and L is shown in fig. 2 for the case of a phantom to image plane separation H of 0·3 cm. Similar curves were obtained for all other values of H used. All of these data indicate a rapid

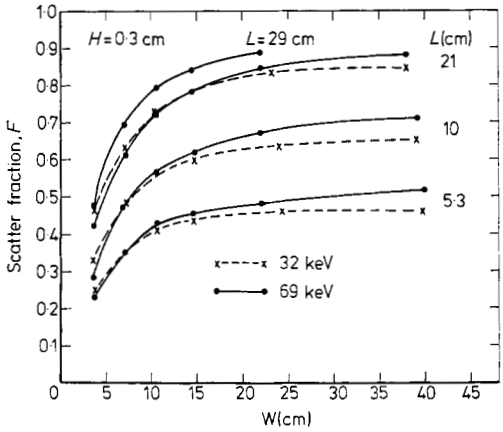

Fig. 2. The scatter fraction F, plotted as a function of the incident beam diameter W, for various polystyrene phantom thicknesses L, and a fixed phantom-to-image-plane separation of 0·3 cm, and for X-ray energies of 32 and 69 keV.

increase in the value of F as W increases from 0 to ~ 15 cm and a levelling-off for larger beam diameters. Also as expected, the scatter fraction increases for increasing phantom thickness. These curves indicate that the use of X-ray beam diameters larger than those needed to cover the area of interest introduces unnecessary scattered radiation which can only degrade the image quality.

Similar curves have also been obtained by plotting the scatter fraction as a function of L for a fixed H and various W values. These curves also exhibit a levelling-off behaviour for L values greater than 15 cm.

3.2. *Dependence of the scatter fraction on the patient to image plane separation*

The dependence of F on the parameter H is shown in fig. 3 for a W value of 25 cm and various L values. Similar data were obtained for all W values used. These data show the scatter reduction that is achieved by increasing the separation distance H. The reduction is seen to be approximately linear in the range from 0 to 25 cm with a slope that is essentially independent of L.

A systematic examination of the data obtained showed that for a given phantom to image plane separation H, the scatter fraction was approximately constant for a given value of the product of the beam diameter and phantom thickness. Fig. 4 gives the scatter fraction F as a function of the product $(L \cdot W)$ for both 32 and 69 keV. These data show that F is approximately independent of X-ray energy in this energy range and the curves provide estimates (approximately within $\pm 10\%$) of the scatter fraction F for all

combinations of these parameters in the diagnostic energy range. For example, for an incident beam diameter W of 20 cm, a patient thickness L of 20 cm and a patient to image plane separation H of 5 cm the scatter fraction F is approximately 0·73.

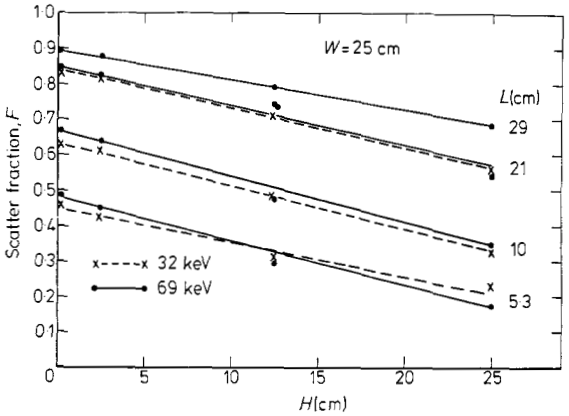

Fig. 3. The scatter fraction F, plotted as a function of the phantom-to-image-plane separation H for various phantom thicknesses L and an incident beam diameter of 25 cm, and for X-ray energies of 32 and 69 keV.

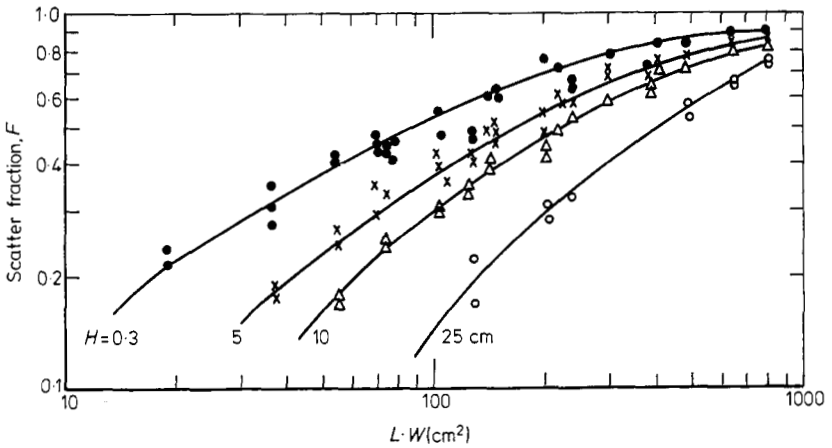

Fig. 4. A general plot of the scatter fraction F as a function of the product of the phantom thickness L and the beam diameter W for different phantom-to-image-plane separation distances H. The solid lines represent an empirical fit to the experimental data with an accuracy of approximately ± 10%.

4. Comparison with previous results

4.1. *Scatter fraction and the geometric parameters*

Fig. 5 gives a comparison of the present results with the experimental measurements of Stargardt and Angerstein (1975) who measured the scatter fraction behind water phantoms as a function of the phantom to image plane

distance. These latter data were obtained with a tube potential of 105 kV_p and a rectangular field of 20 cm × 20 cm. Their results are given for phantom thicknesses of 5·5, 9, 22 and 27·5 cm and exhibit excellent agreement with the present data, except for the 5·5 cm phantom at large phantom-to-image-plane

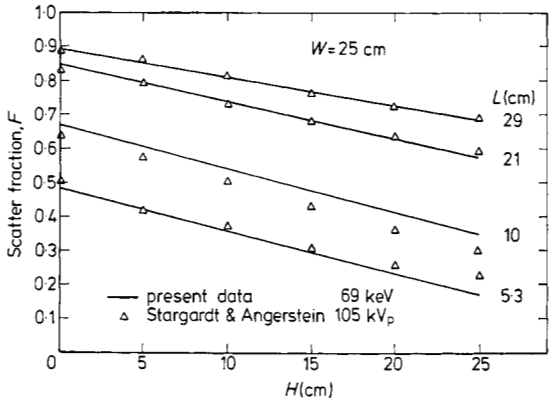

Fig. 5. A comparison of the scatter fraction F, plotted as a function of the phantom-to-image-plane separation with previous experimental measurements made on water phantoms.

separations. These differences may be due to the field size variation in the two experimental geometries which is relatively unimportant for the thicker phantoms.

Reiss and Steinle (1973) and more recently Brueckner (1977, private communication) have calculated values of the scatter fraction F by Monte Carlo methods for low atomic number materials. Fig. 6 shows comparisons of the

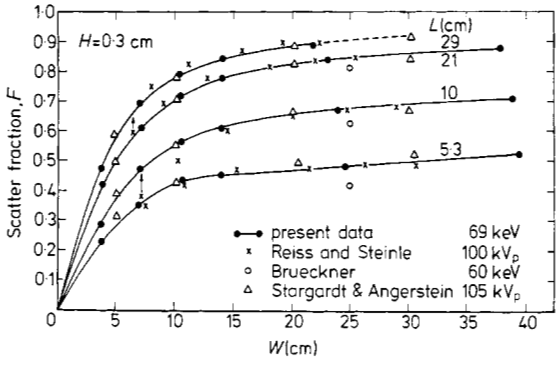

Fig. 6. Comparison of the measured values of the scatter fraction F with Monte Carlo calculations and previous experimental measurements for a phantom-to-image-plane separation of 0·3 cm.

present results with these calculations. In general, the agreement with the Reiss data for water is good, particularly for beam diameters greater than 10 cm. The calculations of Brueckner for polystyrene are slightly lower than the experimental values, particularly for small values of the phantom thickness.

Both calculations are made for the special case of zero phantom to image plane separation.

Fig. 6 also shows a comparison of the present results with the experimental results of Stargardt and Angerstein (1975) which were made for water phantoms with an X-ray tube potential of 105 keV. The phantom thicknesses in these measurements were 5·5, 9, 22 and 27·5 cm and the X-ray beam was confined to a square field of side W. The agreement with the present results for polystyrene is seen to be within 5% over the range of parameters indicated.

Fig. 7 illustrates these calculated and experimental results plotted on a general curve of the type shown in fig. 4. The solid line represents an empirical

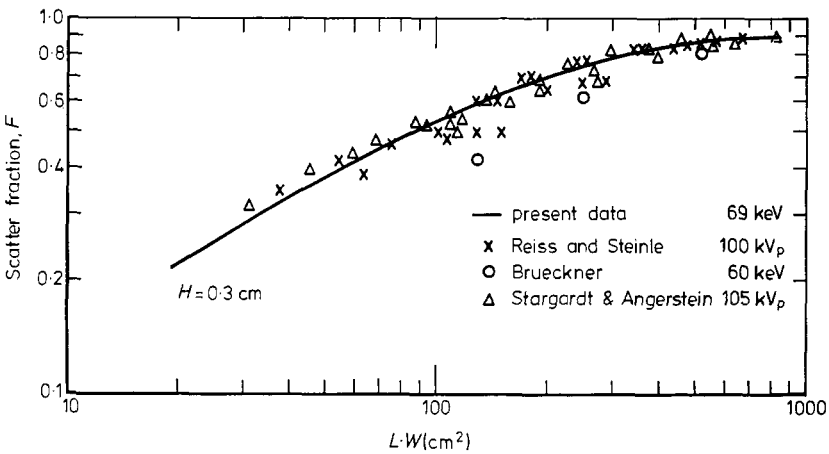

Fig. 7. Comparison of Monte Carlo calculations and previous measurements of the scatter fraction F as a function of the parameter $(L \cdot W)$ with the present measurements for a phantom-to-image-plane separation of 0·3 cm.

Table 2. Comparison of the present results for the scatter fraction F for polystyrene with the results of Goodwin *et al.* (1970) for prestwood phantoms

Beam diameter (cm)	Phantom thickness (cm)	Goodwin (1970)	Present experiments
20	5	0·39	0·46
	10	0·61	0·65
	20	0·82	0·83
35	5	0·50	0·50
	10	0·72	0·70
	20	0·91	0·87

fit to the present data given in fig. 4. The general agreement is seen to be good except for small L values in the 60 keV Monte Carlo calculation.

Table 2 gives a comparison of the scatter fraction obtained for prestwood phantoms by Goodwin *et al.* (1970) for 100 kV_p with 5 mm of aluminium

filtration with the present measurements for an incident X-ray energy of 69 keV and a phantom to image plane separation of 0·3 cm. The experimental values of the scatter fraction for these two measurements show good agreement.

4.2. *Scatter fraction and the incident X-ray energy*

The dependence of the scatter fraction on the incident X-ray energy has been the subject of considerable attention. Previous data have indicated that F increases (Goodwin *et al.* 1970), decreases (Halmshaw 1966, Motz and Dick 1975) or has negligible variation (Reiss and Steinle 1973) as the X-ray energy increases from 30 to 70 keV.

Fig. 8 gives a comparison of the scatter fraction as measured previously (Motz and Dick 1975) for X-ray energies between 30 and 70 keV. As can be

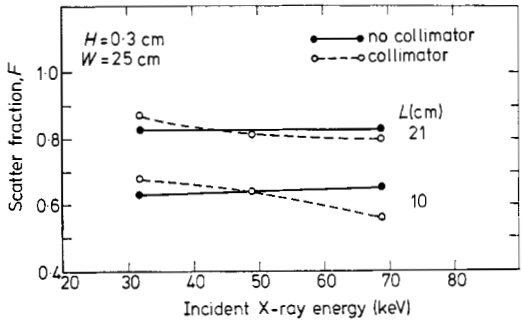

Fig. 8. Comparison of the values of the scatter fraction F measured with and without the optional collimator shown in fig. 1 for polystyrene thicknesses of 10 and 21 cm. The diameter of the incident X-ray beam was 25 cm and the phantom-to-image-plane separation was 0·3 cm.

seen from an examination of the figure, the present data indicate little change in F for this energy region for the specified geometric parameters. In the previous measurements the scatter fraction was measured with a collimator between the phantom and image plane as shown in fig. 1. These results showed a gradual decrease in F as the incident X-ray energy increased from 30 to 70 keV. It now appears that the presence of this collimator introduces a secondary source of scatter into the experimental measurement, particularly at low energies. In addition, the determination of the X-ray fluence in the previous measurements was based on the nomianl area of this collimator which assumes that the detector response does not vary at different points in the incident plane of the detector.

The present data indicate little change in the value of F as the energy is increased from 30 to 70 keV. These results agree with the measurements of Stargardt and Angerstein (1975) who found that the scatter fraction exhibited less than a 10% increase for values of the geometric parameters similar to those given in fig. 8 and for X-ray tube potentials from 60 to 105 kV_p. The present data are still in conflict with the trend observed by Halmshaw (1966) at higher energies which indicates a rapid decrease in F as the incident X-ray energy is

increased. However, it appears that the Halmshaw data include backscattering effects in the scattering medium and, therefore, would not apply to the case where the scatter fraction is evaluated at the image plane. Therefore, the present data support the conclusion that there is less than a 10% increase in the scatter fraction as the incident X-ray energy increases from 30 to 70 keV.

5. Conclusion

We have measured the ratio of the scattered to total X-ray fluence at the centre of the image plane for X-rays transmitted through polystyrene phantoms whose scatter properties approximate those of biological materials. The data show the dependence of this ratio on the principal geometric factors of importance in diagnostic radiology; the X-ray beam diameter, phantom thickness and the phantom to image plane separation. These data, which show good agreement with previous experimental and theoretical data, show less than a 10% dependence on the incident X-ray energy in the region from 30 to 70 keV. The results can be summarised by a simple family of curves which gives the dependence of this ratio on the product of the beam diameter and phantom thickness which may be related to the irradiated volume. These curves provide estimates of this ratio to an accuracy of about 10% over the X-ray energy region and the geometric conditions usually encountered in diagnostic radiology including the use of the air gap technique to reduce scatter effects.

Résumé

Données de dispersion de rayons-X pour le radiodiagnostic

Le rapport de la fluence de rayons-X dispersée à la fluence totale (fraction de dispersion) au centre du plan d'image pour les rayons-X transmis au travers de fantômes polystyrène a été mesuré pour des énergies de rayons-X de 32 et 69 keV, diamètres de faisceaux de rayons-X de 4 à 40 cm, épaisseurs fantômes de 5 à 30 cm et séparations fantômes/plan d'image de 0,3 à 40 cm. Les valeurs expérimentales pour ce rapport accusent une variation de moins de 10% pour ces deux énergies de rayons-X et les données expérimentales révèlent un bon accord avec les calculs de Monte-Carlo et les résultats expérimentaux disponibles pour les matières à numéro atomique réduit. En se basant sur ces résultats, de simples courbes sont produites qui donnent des estimatifs (±10%) de la fraction de dispersion pour toutes les combinaisons de paramètres géométriques rencontrés en radiodiagnostic.

Zusammenfassung

Daten über die Streuung von Röntgenstrahlen für die Praxis der Röntgenstrahlbehandlung

Gemessen wurde das Verhältnis von Streustrahlen zur Gesamtmenge des Röntgenstrahlflusses (d.h. das Streuverhältnis) im Mittlepunkt der Bildebene bei Röntgenstrahlen mit Energiewerten von 32 und 69 keV, die durch Phantome aus Polystyrol hindurchgeführt wurden. Der Durchmesser des Röntgenstrahlbündels betrug 4 bis 40 cm und die Dicke des Phantoms lag im Bereich von 5 bis 30 cm. Der Abstand zwischen dem Phantom und dem Bild lag im Bereich von 0,3 bis 40 cm. Die experimentell gefundenen Werte weisen einen Schwankungsbereich auf, der bei den zwei verschiedenen Energiewerten für die Röntgenstrahlen jeweils unter 10% liegt. Ferner stimmen die Versuchsergebnisse gut mit den Werten der Monte-Carlo-Berechnungen überein. Diese gute Übereinstimmung ist auch mit den experimentellen Ergebnissen, die für Stoffe mit niedriger Atomzahl vorliegen, gegeben. Auf diesen Ergebnissen aufbauend wurden einfache Kurvenverläufe erhalten, die eine Schätzung (±10%) des Streuverhältnisses bei beliebigen Kombinationen der in der Praxis der Röntgenstrahltherapie vorkommenden geometrischen Parameter erlauben.

References

GOODWIN, P. N., QUIMBY, E. H., and MORGAN, R. H., 1970, *Physical Foundations of Radiology* (New York: Harper and Row) Ch. 7.

HALMSHAW, R., 1966, *Physics of Industrial Radiography* (London: Heywood; New York: Elsevier)) p. 142.

HUBBELL, J. H., 1969, *Photon Cross Sections, Attenuation Coefficients, and Energy Absorption Coefficients from 10 keV to 100 GeV*, NSRDS–NBS29 (Washington, DC: U.S. Government Printing Office) p. 72.

MEAKIN, R., 1957, *A Further Handbook of Industrial Radiology* (London: Arnold) p. 43.

MOTZ, J. W., and DANOS, M., 1978, *Med. Phys.*, **5**, 8.

MOTZ, J. W., and DICK, C. E., 1975, *Med. Phys.*, **2**, 259.

REISS, K. H., and STEINLE, B., 1973, *Phys. Med. Biol.*, **18**, 746. (The complete results are given in *Tabellen zur Röntgen diagnostic II*, available from Siemens AG, UB Med, Henkestrasse 127, D-8520 Erlangen, Germany.)

STARGARDT, A., and ANGERSTEIN, W., 1975, *Fortschr. Geb. Röntgenstrahl.*, **123**, 364.